Tensile behavior of flax textile reinforced lime-mortar: Influence of reinforcement amount and textile impregnation

Tensile behavior of Flax Textile Reinforced Lime-Mortar: influence of reinforcement amount and textile impregnation

Giuseppe Ferrara
University of Salerno, Dept. of Civil Engineering, via Giovanni Paolo II n.132, 84084 Fisciano (SA), Italy.
e-mail: giferrara@unisa.it

Marco Pepe
University of Salerno, Dept. of Civil Engineering, via Giovanni Paolo II n.132, 84084 Fisciano (SA), Italy.
e-mail: mapepe@unisa.it
TESIS srl, via Giovanni Paolo II n.132, 84084 Fisciano (SA), Italy.
e-mail: m.pepe@tesis-srl.eu

Enzo Martinelli
University of Salerno, Dept. of Civil Engineering, via Giovanni Paolo II n.132, 84084 Fisciano (SA), Italy.
e-mail: e.martinelli@unisa.it
TESIS srl, via Giovanni Paolo II n.132, 84084 Fisciano (SA), Italy.
e-mail: e.martinelli@tesis-srl.eu

Romildo Dias Tolêdo Filho
Federal University of Rio de Janeiro, Civil Engineering Department, COPPE, P.O. Box 68506, CEP 21941-972, Rio de Janeiro – RJ, Brazil
e-mail: toledo@coc.ufrj.br

Corresponding author: e.martinelli@unisa.it

ABSTRACT

Companies and practitioners working in the civil construction sector are more and more aware and motivated to develop and adopt sustainable building materials, possibly obtained from renewable and locally available resources. As part of this common effort, special attention is being paid to an emerging class of materials generally referred to as bio-based composite systems.

In this context, this paper investigates the mechanical properties of a Textile-Reinforced Mortar (TRM) system produced with Flax textile embedded within a hydraulic lime-based mortar. The research aims at revealing the influence of either the reinforcement amount and the applied pre-treatment of the textile on the resulting tensile response and the cracking patterns exhibited by these TRM systems. The analysis of the results presented herein allows to have a comprehensive overview of the feasibility of using flax textiles for strengthening a retrofitting of existing structures.

KEYWORDS:

Textile Reinforced Mortars, Plant-fibers, Fiber treatment, Crack formation

1.INTRODUCTION

Existing masonry buildings are generally characterized by a significant vulnerability, notably toward seismic events, which requires great attention from both practitioners and researchers in the field of structural engineering [1][2].

In the last decades, the use of composite systems became more and more common in strengthening intervention, as they established themselves among the most attractive retrofitting techniques [3]. Basically high-strength fiber fabrics or grids are attached through either organic (polymeric) or inorganic (mortar-based) matrices on the external faces of existing elements [4][5].

Among the composite systems, Textile Reinforced Mortars (TRMs), produced by adopting cement- or lime-based mortar matrices, are particularly suitable for strengthening masonry elements, due to their mechanical properties and to the material affinity to the materials traditionally adopted in existing constructions [6][7]. Several other acronyms, such as Fabric Reinforced Cementitious Matrix (FRCM), Textile Reinforced Concrete (TRC), Cementitious Matrix Grid (CMG), Inorganic Matrix Grid (IMG) or Composite Reinforced Mortar (CRM), are adopted in the literature to define the same kind of inorganic-matrix composite systems [8].

The use of TRM systems is considered to be an efficient, practical, and cost-effective solution for seismic retrofitting and repair of structures. This popularity lies in the reversibility and versatility of the interventions, with a wide selection of solutions combining large numbers of fabrics and mortars available on the market [9].

Several experimental studies were carried out in order to respond to the need for a comprehensive definition of TRM mechanical behavior and for qualification procedures [10]. Tensile tests on composite samples and shear bond tests on composite strips applied to masonry substrates were carried out by adopting different reinforcement solutions comprising carbon [11], steel [12], glass [13][14], basalt [15][16] and PBO fiber grids [17][18]. Significant attention was also paid to

assessing the durability of TRM systems, with the aim to define the mechanical properties of the composite in the long term and under the exposure to environmental actions [19][20][21].

During the last decades, the awareness towards environmental issues has been increasing significantly, as the mitigation of environmental impacts of human activity is getting more and more relevant in all the industrial fields. Among the others, also in the building sector, "greener" solutions are being implemented with the aim to reduce the demand of energy, the use of raw materials and the emission of green-house gases [22][23][24][25].

The use of plant fibers in composite systems, in lieu of industrial ones, represents a promising solution to implement low environmental impact materials, falling within the class of the bio-composites. Dicker *et al.* [26] carried out a comprehensive comparative analysis on the use of "green" conventional composites, taking into account several aspects, such as density, strength, cost and embodied energy. It was found that, for composite systems of similar mechanical performance, in absolute terms, the embodied production energy of synthetic fibers is ten times higher than natural fibers, whilst the production of synthetic composites requires around five times more energy than green ones.

Therefore, several studies were carried out to investigate the mechanical properties of mortar-based composites comprising several types of plant fibers, such as jute, sisal, coir, flax, hemp, and curaua [27][28][29]. Pull-out tests of the fiber yarns from the matrix were carried out to analyze the bond behavior at the textile-to-mortar interface [30]. TRM specimens and TRM strips bonded on masonry substrates were implemented with the aim to investigate the tensile and shear-bond responses [31]. The efficiency of natural (plant-fiber based) TRMs as external strengthening systems of masonry elements was investigated by means of tests at the structural scale aiming at assessing both the in-plane shear capacity, by means of diagonal compression tests [32] [33], and the out-of-plane flexural strength, by means of eccentric load compression tests [34]. The experimental investigations showed a promising mechanical response of Natural TRM composite systems, in several cases with a good exploitation rate of the entire dry textile strength. Moreover, mechanical

tests on structural elements showed a significantly beneficial influence of the composite system on the overall capacity of the composite member. However, few discrepancies were observed with respect to the mechanical response of conventional TRMs. The tensile response of Natural TRM systems was characterized by large deformations, with a transition zone between the first elastic branch and the final hardening response characterized by a significant drop in load corresponding to the occurrence of cracks due to the highly different stiffness values between textile and mortar [35]. Consequently, also the developed crack openings attained significant values. As expected, the reinforcement volume ratio controls the efficiency of Natural TRMs, with a significant enhancement of the mechanical tensile strength for values higher than 3 % [36].

Conversely, several drawbacks were observed also in terms of durability mainly due to the high sensitivity of plant fibers to the aggressive alkaline environments of either cement- or lime-based mortars [35][37][38][39]. Few treatments were proposed in the literature to address both mechanical and durability issues related to the use of plant fibers in TRM composites. The use of coating systems, for instance by epoxy resins, may serve to protect the fibers from the alkaline attack preventing the direct contact with the mortar and, at the same time, as a bond promoter enhancing the mechanical response [31][32]. Polymeric treatments of plant fibers may improve both tensile strength and stiffness of plant fibers [39]. Hornification processes, comprising of hot water washing cycles, which reduce the cross section of fibers, may lead to similar improvements in terms of tensile response [40]. Alkali treatments, based on fibers immersions in calcium hydroxide solutions, entails the removal of the external layers of the fiber structure (hemicellulose and lignin from fiber wall), and the increase of the roughness by calcium deposition, resulting in a positive influence on the fiber-to-matrix bond [40].

The present study aims at investigating the tensile behavior of Natural TRMs made of flax textile and hydraulic-lime mortar matrix. Specifically, the experimental analysis was conceived to influence the composite efficiency from two different aspects. At first, the influence of the textile volumetric reinforcement ratio was studied by implementing two reinforced configurations

comprising either of one or two layers of flax textile. Then, the effect of a polymeric impregnation treatment of the textile was observed by performing TRM composites comprising either of one or two layers of impregnated flax textile.

The paper confirms the promising performance of Natural TRMs, as they represent a technically competitive, environmentally and economically advantageous alternative to the conventional composite systems. Moreover, it shows that significant improvements in the mechanical response can be obtained in terms of both capacity and crack pattern developed in tension.

2.MATERIALS AND METHODS

2.1 Textile

The textile reinforcement employed for producing the TRM composites analyzed hereafter consists of a bi-directional flax fabric (commercialized by the "Innovation s.r.l." company and labelled FIDFLAX Grid 300 HS20 ® [41]) characterized by a grid comprising of 4.3 yarns per centimeter (in both directions) and a clear opening size of about 3 mm (see **Figure 1**). The yarns of the flax textile are characterized by an average cross section equal to 0.25 mm^2 (coefficient of variation "*cv"* equal to 17 %), tensile strength of 354 MPa (*cv* = 11 %), elastic modulus of 9.4 GPa (*cv* =7%) and strain at failure of 5.6% (*cv* =10 %) [38]. In addition, each elementary flax filament constituting the yarn presents an average nominal diameter equal to 16 μm (*cv* 29 %) and a density of 1.2 g/cm^3.

The flax textile was employed in both non-impregnated and impregnated conditions. As a matter of principle, one of the main issues related to the use of natural reinforcement is its geometric stability during casting, which can be compromised due to the high flexibility of these types of reinforcement [36]. For these reasons, textile impregnation would be desirable and, it is more and more common to employ this kind of natural reinforcement in either lime- or cement-based mortars. In fact, this treatment mitigates a loss of geometric stability and, in some cases, enhances the bond between matrix and reinforcement, and increases the durability of the natural composite system [31].

In the present research, the impregnation treatment was based on applying a polymer coating on the flax textile. Specifically, the coating substance (XSBR Latex, commercial name "NTL-218" produced by Nitriflex [42]) consisted in an aqueous solution with a *styrene-butadiene* polymer characterized by a solid content of 49 ± 1 % of weight, a pH of 9 ± 0.5 and a viscosity of 50-350 mPas. The *styrene butadiene* polymer was adopted since beneficial effects were observed, both in terms of tensile strength and bond adherence with the matrix, when applied on plant fibers filaments [39]. The treatment was carried out by brushing the substance on flax fabric portions of 350 x 600 mm^2 (**Figure 2a**). During the treatment, the textile was arranged in wood frames to guarantee a correct

tensioning of the yarns. The flax textile portions were treated at ambient temperature conditions (**Figure 2b**) then released of the excess liquid and dried in a ventilated chamber for 24h at a controlled temperature of 38 ± 2 °C and with a wind velocity of 0.5 m/s. Finally, impregnated flax strips (60 mm large) were cut from the treated textile (**Figure 2c**).

The textile reinforcements were mechanically characterized by means of tensile tests carried out on the following two series of specimens:

- *Flax Textile*: comprising 5 specimens of 60 mm large and 500 mm long flax textile strips (containing 12 flax yarns);
- *Impregnated Flax Textile*: comprising 5 specimens of 60 mm large and 500 mm long polymer coated flax strips (containing 12 flax yarns);

The tensile tests were carried out in a Shimadzu (model AG-Xplus) universal testing machine, characterized by a 10 kN maximum load capacity, with a displacement control (4 mm/min) [38]. Two aluminum plates were glued to each edge of the specimen for a length of 100 mm, leaving a gauge length of 300 mm. Extensometer was placed at mid-length to detect the elongation of the strips during the test, over a length of 200 mm (**Figure 3**). The textile mechanical characterization was conducted according to the standard ISO 13934-1 [43].

2.2 Mortar

The composites analyzed in the present research were prepared by employing hydraulic lime-based mortars (commercialized by the Italian company "Innovation s.r.l." and labelled FIDCALX NHL5 ® [44]). Several studies demonstrated a good efficiency of lime-based composite systems for strengthening and retrofitting existing masonry structures [9].

The hydraulic lime-based mortar consisted of a premixed matrix with pure natural hydraulic lime binder and selected fine aggregates with a maximum nominal diameter equal to 1.19 mm [30]. The granulometric distribution of the whole particles guaranteed an adequate penetrability of the mortar within the textile, where the clear opening of the grid was more than 2 times higher than the

maximum aggregate size. The mortar was produced with an amount of water equal to the 19 % by weight of the pre-mixed dry mixtures (i.e., binder and aggregates): the resulting water-to-binder ratio of the mixture was equal to 0.60.

For each casting batch, the key properties of the mortar were measured at both the fresh and hardened states. More specifically, flow table tests were performed at fresh state (here, the consistency is expressed in terms of mean diameter d^* of the mortar after jolting the table 15 times [45]) and compressive (f_c) and flexural (f_f) strengths at the hardened state in accordance with EN 196-1 [46]. The results of these tests, as well as the number of the tested samples, are summarized in **Table 1**.

2.3 Flax Textile Reinforced Mortars

The experimental campaign reported hereafter was aimed at analyzing the role of several parameters governing the mechanical response of the resulting flax TRM composites, such as:

- number of textile layers embedded within the composite;
- the application of the flax textile impregnation treatment;

Therefore, the following four series of specimens were produced (**Table 2**):

- *Flax TRM-1L*: composites produced with one layer of flax textile embedded in hydraulic lime mortar;
- *Flax TRM-1L-imp*: composites produced with one layer of impregnated flax textile embedded in hydraulic lime mortar;
- *Flax TRM-2L*: composites produced with two layers of flax textile embedded in hydraulic lime mortar;
- *Flax TRM-2L-imp*: composites produced with two layers of impregnated flax textile embedded in hydraulic lime mortar;

Each specimen was cast in its own mold by alternating layers of mortar to layers of textile as schematized in the images proposed in **Figure 4**. Each flax strip was arranged by clamping the two

edges to make the fabric as taut as possible. For impregnated flax strips this procedure was not necessary as the textile already had been stretched during the coating treatment. The grid was pressed by means of a roll to ensure a proper penetration of the mortar within the mesh clear opening spaces.

The produced Flax TRM samples present a nominal length and width equal to 500 mm and 60 mm, respectively. Nevertheless, each series was characterized by its specific thickness as the average thickness of the specimens varied for each series depending on the number of textile layers, the type of textile and the type of mortar. For instance, the series of specimens comprising of non-impregnated flax textile were characterized by a thicker cross section, compared to specimens characterized by the same number of plies with impregnated textile. This is due to the "stretching" process of the textile during the manufacturing process that made it harder the specimen casting, with consequent higher amounts of mortar to guarantee a correct implementation of the composite. **Table 2** reports the number of the tested samples and summarizes the average properties differing for each series, where t_{mean} represents the average thickness of the specimen of the series, A_{text} the area of the textile comprised in the cross section, and ρ represents the reinforcement ratio equal to the ratio between the area of the textile and the area of the composite cross section.

All the produced samples were tested in a Shimadzu (model AG-Xplus) universal testing machine with a maximum load capacity of 10 kN and a displacement control of 0.3 mm/min, in accordance with [10] (**Figure 5**). Each specimen is characterized by a 300 mm gauge length and, for performing the tests, two aluminum plates were glued at each edge of the specimen over a length of 100 mm, and connected to the loading machine by means of a bolt (see **Figure 5**), in order to transfer the tensile load to the specimen by shear stresses without clamping the specimen edges (clevis configuration) [47].

The external surface of the specimens (60 mm x 300 mm) was treated by painting a white background on which black dots were stochastically sprinkled, in order to get images for a Digital Image Correlation (DIC) analysis (see **Figure 5c**). Photos were captured by a camera placed at a focal

1 distance of 50 cm. The acquisition rate was of 3.75 photos/min and the resolution of the photos was
2 of 4310 x 2868 pixels (0.08 mm/pix).

3.RESULTS AND ANALYSIS

3.1 Tensile behavior of Flax-Textile reinforcements

Figure 6 reports the stress-strain curves for both *Flax-Textile* and *Impregnated Flax-Textile* strips subjected to tensile loads. The main parameters describing the textile tensile response are summarized in **Table 3** where P_{max} represents the maximum load, while δ_{max}, σ_{max} and ε_{max} are the axial displacement, stress and strain corresponding to the maximum load, respectively. Moreover, the elastic modulus E is evaluated as the slope of the stress-strain curve in the branch comprised between 50 % and 80 % of the tensile strength (σ_{max}) for each curve.

The curves shown in **Figure 6** highlight that the tensile response of both *Flax-Textile* and *Impregnated Flax-Textile* strips can be divided into two different stages: a first branch in which high deformation is registered and a subsequent more rigid and quasi-linear branch up to failure.

The untreated *Flax Textile* strips show a first branch with a significantly low stiffness increasing up to a quasi-linear response before failure (grey curves in **Figure 6**). The high deformability of the strips at low strain level can be attributed to the peculiar geometric arrangement of the fabric. In fact, the textile is made of yarns comprising several flax filaments that are randomly distributed within the section, with some of them not oriented in the direction of tensile stresses: they need an initial displacement to be stretched and start contributing to the axial stiffness. Moreover, the textile strip includes 24 yarns that are, unavoidably, not uniformly subjected to the same stress level, with a consequent heterogeneous distribution of the tensile stresses among the bundle. The failure mode is characterized by a progressive rupture of the flax yarns, occurring for each one in a random section along the free length of the specimen.

Similarly, the *Impregnated Flax-Textile* strips also show a first stage in which the stiffness is lower than the quasi-linear branch up to failure of the textile. However, the initial stiffness is slightly higher than the one observed for untreated textiles. This is certainly due to the beneficial effect of the coating treatment: on the one hand, the stretching of the textile during the impregnation

implementation oriented a higher number of fibres in the tensile direction and, on the other hand, the coating polymer created a link among the filaments leading to a more uniform distribution of the stress among the flax yarns (**Figure *7***).

It is worth mentioning that the *Impregnated Flax Textile* strips exhibited a tensile strength approximately 20 % lower than the companion untreated flax grid. This evidence is attributed to the fact that, as also demonstrated in a previous research [30], the impregnated textile behaves as a "polymeric composite" (see also **Figure *7***) in which the amount of coating substance strongly governs the failure mode, characterized by a progressive simultaneous sliding of the filaments within the yarns, rather than by an abrupt rupture of the bundles, which is observed for the untreated textile.

In terms of stiffness, no significant differences were observed for both untreated and impregnated textiles in the quasi-linear branch. The lower value of strain at failure observed in the *Impregnated Flax-Textile* strips is due to both the more "rigid" behavior at low strains and the lower tensile strength. As a matter of fact, the impregnation treatment, although slightly reducing the tensile strength of the textile, resulted in a beneficial effect on the coated grid as the yarns were sufficiently stretched already in the unstressed configuration: this phenomenon increases the capacity of exhibiting higher tensile stresses at low strain values and confers an overall lower deformability to the impregnated fabrics.

Tensile stress-strain response of *Flax-Textile* series was characterized by s significant variability. This aspect, typical of plant fibres textiles, is due to the nature of the flax filaments, and to their arrangement within the threads [38].

3.2 Tensile response of Flax-TRMs

The stress-strain curves obtained for the tested composites are summarized in **Figure 8** for the TRM reinforced with either 1 and 2 layers of flax grids. It is worth mentioning that the axial stresses were evaluated by considering them uniformly distributed over the entire composite cross section and,

similarly, the axial strain was computed as the mean deformation of the composite over the entire gauge length (equal to 300 mm as described in section 2.3).

The curves plotted in **Figure 8** show that the typical response of TRM specimens subjected to tensile loads is characterized by a tri-linear behavior in which three stages can be identified:

- *Stage I* in which the mortar is uncracked, and the response is linear up to the occurrence of the first crack, corresponding to the achievement of the axial stress equal to the mortar tensile strength;
- *Stage II* characterized by a multiple crack development: the number of the cracks, the distance between them and the crack openings depend on several aspects such as the mechanical properties of either textile and mortar, the interlocking behavior between fibers and matrix, the textile reinforcement ratio, the geometry of the specimens and the boundary conditions reproduced during the test;
- *Stage III* which starts once the crack pattern has completely developed and it is characterized by a nearly linear branch up to the failure: the response in the *Stage III* is mainly governed by the textile and the stiffness of the composite assumes values similar to that of the fabric alone tested in tension [10].

Two failure modes can be observed [10]:

- rupture of the textile in a casual cross-section in proximity of one of the gauge length edges (*mode A*);
- slipping of the textile in the anchored zones (*mode B*).

The stress-strain curves reported in **Figure *8*** can be identified by means of some relevant parameters such as normal maximum stress σ_{max}, the strain at failure (ε_{max}) corresponding to the maximum load (P_{max}) and maximum displacement (d_{max}) respectively, and, the maximum stress achieved in the textile at failure ($\sigma_{max,text}$) and the failure mode (either A, or B). The average value, as well as the coefficient of variation (*cv*) obtained in the present study, are summarized in **Table 3**.

Moreover, **Figure *9*** reports the average values obtained for the following relevant parameters identifying the overall response of TRM subjected to tensile loads:

- the parameter σ_1, which represents the stress corresponding up to the occurrence of the first crack, at the transition point between *Stages I* and *II* (see **Figure *9*a**);
- the parameter ε_2, which represents the main value of the strain corresponding to the transition point between *Stages II* and *III* (see **Figure *9*b**); the transition point between *Stages II* and *III* corresponds to the point in which a remarkable change in the stress-strain curve slope occurs, notably at the end of the crack development process;
- the exploitation ratio, defined as the ratio between the maximum stress within the textile achieved during the test and its tensile strength ($\sigma_{max,text}/f_{t,text}$ in **Figure *9*c**), which is an important parameter quantifying the efficiency of the composite system.

3.2.1 Influece of the number of textile layers

The stress-strain response concerning the series *Flax TRM-1L* (**Figure *8*a**) is characterized by a first linear branch followed by either one or two significant drops in load, corresponding to the occurrence of cracks in the matrix. A premature failure mode occurred due to a slipping of the textile in one of the gripping areas of the specimens.

The stress-strain curves concerning the series *Flax TRM-2L* (**Figure *8*b**) exhibited a behavior comparable to the typical tri-phase response of TRMs in tension described in Section 3.2. For this series, the failure mode was characterized by the tensile failure of the textile in one of the sections in proximity of the plates in the gripping area. Unavoidably, due to absence of clamping systems at the edges of the specimens, a partial slipping of the textile in the gripping areas must have occurred as well.

In both series a significant drop in load was observed in correspondence to the occurrence of a crack within the matrix. This behavior, in line with similar studies on TRM composites in which plant

fibers were adopted as reinforcement [35][36], diverges from the typical response of TRMs in which conventional reinforcing textiles are adopted. This is attributed to both the lack of straightness of the textile (especially in the case of no treatment) and the lower stiffness of plant fibers. Consequently, at low strain levels, the load is mainly borne by the mortar, which leads to premature crack formation in the mortar matrix.

The experimental results showed that by increasing the reinforcement ratio (ρ) from 1.3 (for *TRM-1L*) to 2.3 (for *TRM-2L*), the resulting TRM tensile response changes, moving from a failure mode due to the slip of the textile in the gripping areas (*mode B*), to the tensile failure in the reinforcement (*mode A*). This gain of efficiency can be appreciated in terms of fiber exploitation that attained a value of 36 % in the series *TRM-1L* and 60 % in the series *TRM-2L* (see **Figure *9*c**).

With respect to the series *TRM-2L*, although the rupture of flax yarns occurred, the maximum average stress in the textile was lower than its tensile strength. Such a discrepancy is due to the different loading conditions of the textile when tested on its own and when it is restrained by the surrounding mortar. Moreover, a local slippage of the textile at the edges of the TRM samples may have occurred, whereas in the case of the sole textile tested in tension, the use of resins to anchor the strips prevented such a phenomenon

The normal stress corresponding to the first crack (σ_1) was higher in strips with more textile layers (**Figure *9*a**). This parameter is related to the tensile strength of the matrix, which can be assumed in the range of 2.1÷2.8 MPa. In both series, the mean value of σ_1 was lower than the tensile strength of the mortar. This evidence is attributed to the fact that the presence of the textile within the composite creates a local concentration of stresses in proximity of the fiber yarns, with a consequent discrepancy with the ideal uniaxial direct tensile conditions. This local effect seemed to be more relevant in *TRM-1L* series than in the *TRM-2L* ones. As a matter of fact, a wider spread arrangement of the textile within the composite creates a more uniform distribution of the normal stresses through the cross section.

In terms of maximum load capacity P_{max}, a significant increase was observed: a maximum load of 3.3 times higher was attained in the *TRM-2L* series when compared to the *TRM-1L* ones (**Table 4**). This aspect highlighted that the mechanical behavior of the composite, notably the failure mode, can be changed by increasing the amount of textile, hence leading to a more efficient composite system.

The stress-strain curves for either the Flax *TRM-1L-imp* (**Figure *8*c**) and Flax *TRM-2L-imp* (**Figure *8*d**) highlight that, due to the lower stiffness of the textile (with respect to the mortar) at low strain levels, the *Stage II* was characterized by a significant drop in load corresponding to the occurrence of a crack within the matrix. In both series the failure occurred with the rupture of the textile yarns (*mode A*).

One of the specimens of the series Flax *TRM-2L-imp* was characterized by a significantly stiffer stronger response when compared to the other specimens. This behavior can be directly attributed to the impregnation treatment adopted. Specifically, the impregnation treatment was manually carried out and applied on several textile portions. Such procedure, adopted without having at disposal standardized industrial techniques, unavoidably led to a heterogeneity among the textile strips. In fact, as shown in the literature relatively small difference in the coating thickness may produce strong effects in the final performance of the textile [48]. In order to reduce the influence of such variability in the composite behavior, the TRM specimens were prepared by uniformly distributing the flax strips deriving from the different portions, among the various specimens and series. The better performance exhibited by this specimen can be attributed to the use of flax strips characterized by an impregnation treatment realized in a more efficient manner.

By comparing the average values of the strains ε_2 and ε_{max} in **Figure *9*b**, no significant differences are observed, highlighting the fact that although increasing the fiber reinforcement ratio ρ from 1.6 to 2.5, no significant changing is obtained in terms of stress-strain response. This is also confirmed by referring to the main value of the fiber exploitation ratio as equal to 67% and 65% for the *TRM-1L-imp* and *TRM-2L-imp* series (**Figure *9*c**), respectively. In terms of the normal stress

corresponding to the first crack σ_1 it increased by increasing the number of textile layers (**Figure *9*a**). This trend, in line with what was observed in the non-impregnated textile TRM specimens, can be explained with the same considerations discussed for those series. With respect to the capacity of the composite in terms of maximum load P_{max}, a value of about two times higher was obtained by doubling the amount of textile (**Table 4**). The linear relationship between the reinforcement amount emphasizes that, in the case of the impregnated textile, the fiber reinforcement ratio ρ of the Flax *TRM-1L-imp* series was enough to properly exploit the strength of the composite, leading to the same failure mode of the specimens of the series *Flax TRM-2L-imp*.

3.2.2 Influence of textile impregnation treatment

The stress-strain response of Flax *TRM-1L* (**Figure *8*a**) and Flax *TRM-1L-imp* (**Figure *8*c**) series emphasized a different mechanical behavior of the two systems showing that the use of impregnated textile affected the mechanical behavior in tension. Flax *TRM-1L* specimens are characterized by the development of either one or two cracks (**Figure *8*a**), and by a failure mode due to the loss of textile-to-matrix bond in the gripping areas, while Flax *TRM-1L-imp* specimens are characterized by a clear three-phases response with a much higher number of cracks developed in the *Stage II*, and a failure mode with the rupture of the textile (**Figure *8*c**).

The use of impregnated textile led to a general improvement of the mechanical response of the composite. The maximum load capacity P_{max} of the *TRM-1L-imp* series was 1.5 times higher than the mean value concerning the *TRM-1L* series (**Table 4**). The beneficial effect of the impregnation can also be appreciated in terms of the exploitation ratio, that assumed a value of 1.9 times higher in the TRM reinforced with the impregnated textile when compared to the reference one (**Figure *9*c**).

In terms of normal stress corresponding to the first crack σ_1, a significant reduction of about 37% is observed in the series reinforced by the impregnated textile with respect to the reference one (**Figure *9*a**). This evidence can be explained by the tensile stress-strain response of the textile (**Figure 6**) in which it can be observed that being equal the strain, the impregnated textile is capable to bear a

higher load. Therefore, it can be asserted that in the *Stage I* the contribution of the impregnated textile in the TRM is more significant than that exhibited by the dry textile. As a consequence, the phenomenon of local concentration of normal stresses in the proximity of the textile is more pronounced in the TRMs with impregnated textile with a consequent occurrence of the first crack at lower stress values.

Regarding the TRM with 2 textile layers, the Flax *TRM-2L* (**Figure *8*b**) and Flax *TRM-2L-imp* (**Figure *8*d**) series show a stress-strain curve characterized by the three stages, in which the occurrence of cracks causes significant drop in loads and the failure occurs with the tensile rupture of the textile in a section in proximity of the gripping area. P_{max} value was about 10% lower in the *TRM-2L-imp* series when compared to the *TRM-2L* one (**Table 4**). This is due to the lower tensile strength of the impregnated flax textile with respect to the dry textile. Indeed, the two systems showed similar efficiency in terms of exploitation ratio, with a main value of 59% and 65% respectively for the series *TRM-2L* and *TRM-2L-imp* (**Figure *9*c**).

The series of specimens reinforced by the impregnated textile exhibited a mean value of the stress corresponding to the occurrence of the first crack of about 30 % lower than the reference series (**Figure *9*a**). This result is in line with what had been observed in the series of specimens reinforced by one layer of textile and may be explained with the same considerations made for them.

The *TRM-2L-imp* specimens exhibit a higher number of cracks developed at lower strain levels. The average value of ε_2 was much lower in the composite reinforced with the impregnated textile of about 45% (**Figure *9*b**). Moreover, the load drop corresponding to the occurrence of a crack was much lower in *TRM-2L-imp* specimens than in the *TRM-2L* ones. These aspects are due to a stiffer response of the impregnated textile at lower strain, with respect to the dry flax textile, and to a better fiber to mortar bond behavior provided by the impregnation.

As a general consideration on the effects of the impregnation treatment, by comparing *TRM-2L* and *TRM-2L-imp* series, characterized by the same failure mode, the results concerning the specimens with the coating treatment present larger variability (Table 4). This experimental evidence is due to

the coating strategy adopted resulting in a non-uniform level of impregnation for all the textile strips. In fact, according to the literature, thicker coating layers may hinder the full exploitation of the bundles' tensile strength (due to a telescopic failure), and promote softening plastic behaviours of the composite [48]. Therefore, it is worth emphasising that although the textile treatment causes a general beneficial effect on the tensile behaviour Flax-TRMs, in order to make the material suitable for applications a more reliable coating strategy is needed.

3.3 Analysis of the crack pattern

The present section analyses the crack development on Flax TRMs during the tensile tests, which provides relevant information about the actual efficiency of Flax TRM composites systems.

3.3.1 Crack spacing

An overview of the crack formation patterns in the tested TRM systems is presented in **Figure *10***: in accordance with the results discussed in the previous section. It is remarked that the number of cracks (which, in principle, is related to both the quality of the adhesion between matrices and fibers and the amount of reinforcement [49]) increases by both increasing the numer of textile layers as well as by impregnating the flax textiles.

Furthermore, a more fundamental analysis is presented based on the Digital Image Correlations (DIC) analysis executed during the tensile tests. A representative example of this analysis is shown in **Figure 11**. The implementation of a DIC analysis leads to identifying the load level at which cracks open, the evolution of crack numbers (and, hence, average spacing) and their width development up to failure. **Figure 12** shows, for each series, the evolution of crack spacing during the tests in correlation with the axial strain.

Significant differences are observed in terms of crack developments between the two series of TRM with 1 textile layer (**Figure 12a**). *TRM-1L* specimens are characterized by the formation of either one or two cracks, while *TRM-1L-imp* specimens are characterized by a well-defined *Stage II* in which several cracks develop. Moreover, the load drop corresponding to the occurrence of a crack

is far less significant in the *TRM-1L-imp* specimens than those of the reference series. **Figure 12a** clearly shows this different behavior. Due to the development of several cracks developed at lower strain values, the average crack spacing of *TRM-1L-imp* specimens steeply decreases when compared to that of the *TRM-1L* specimens. This aspect, together with a less significant drop in load corresponding to each crack occurrence, makes the *TRM-1L-imp* specimens behaving more efficiently as a composite system when compared to the *TRM-1L* specimens in which the tensile response seems to be alternatively exhibited by either the textile or the matrix, rather than by the entire composite system.

The analysis of the crack pattern presented in **Figure 12b** also emphasizes the lower deformability of the *TRM-2L-imp* composites. The group of curves representing the crack spacing as a function of the axial strain, concerning the *TRM-2L-imp* series are characterized by a steeper trend with a closer crack spacing, indicating the higher number of cracks developed. Also, the use of the impregnated textile leads to developing a denser crack pattern (**Figure *10***), which occurs at lower strain values, anticipating the beginning of the *Stage III*, in which the composite is supposed to contribute to the strength of the reinforced structural element.

3.3.2 Crack width

Another fundamental parameter that points out the efficiency of TRM composite systems is the average crack width. In view of feasible applications of the TRM composite for structural elements retrofitting and strengthening, it is important to focus the attention on the crack pattern. The crack openings expose the textile to the external environment conditions and, hence, represent a relevant aspect for the durability of the whole composite system.

As already mentioned, the crack width was evaluated through a DIC analysis, but, due to the peculiarity of the TRM analyzed in the present research, a simplified approach is presented herein to estimate the average value of the crack width for each specimen. Specifically, the mean crack width (w_m) at each strain stage (ε) can be evluated by adopting the following equation:

$$w_m(\varepsilon) = \frac{(\varepsilon - \varepsilon_1)}{n_{cracks,\varepsilon}} \cdot L \qquad \text{with } \varepsilon_1 < \varepsilon < \varepsilon_{\max} \tag{1}$$

where ε_1 is the strain value at the transition point between *Stages I* and *II*, L is the free length of the specimen, $n_{cracks,\varepsilon}$ is the number of cracks developed along the free length at the generic deformation stage (ε). This relationship was obtained by assuming that the entire elastic deformation of the matrix to be exploited during the *Stage I*, and that in the next Stages *II* and *III*, the axial displacement is entirely due to the deformation of the textile. This assumption well suits the case in which the flax textile is characterized by a significantly lower stiffness with respect to the hydraulic lime mortar matrix. The accuracy of the adopted procedure is confirmed by comparing the average crack width development obtained with both the presented eq. (1) and the DIC analysis (**Figure 13**).

Figure 14 reports the curves obtained by eq. (1) for each specimen as a function of the corresponding axial strain. The crack width of the *TRM-1L-imp* specimens is much lower than that exhibited by the *TRM-1L* specimens (**Figure 14a**). This is due to the lower deformability of the impregnated textile, and to the development of a higher number of cracks. The curves plotted in **Figure 14b** for the *TRM-2L* and *TRM-2L-imp*, yet emphasizing a variability in the results concerning the two series, show that the group of specimens in which the impregnated textile was adopted are characterized by crack openings lower than those exhibited by the *TRM-2L* specimens. It is worth to mention that although the two series of specimens failed in *mode A*, a significantly beneficial effect was provided in terms of crack opening by adopting the impregnated textile.

Finally, a more comprehensive overview of the results achieved herein is presented in **Figure 15** where the mean curve for each series is plotted both in terms of the number of cracks per linear meter and crack width as a function of the corresponding axial strain. This figure represents the first step toward a rational practical approach for evaluating the feasibility of using Flax TRM composites for masonry retrofitting and strengthening.

3.4 Bond of Flax textile embedded in lime-based mortar

The analysis of the crack pattern led to estimate the average bond stress occurring between the flax textile and the surrounding lime-based mortar. As a matter of the principle, it can be assumed that through the specimen length the applied force (F) is partially borne by the mortar and the textile reinforcement: in fact, by considering the portion of specimen between two consecutive cracks, it can be also assumed that the load is entirely supported by the textile in proximity of the cracked section, where the contribution of the mortar is null as the matrix is broken (**Figure 16**). Then, moving towards the centre of the cracked composite, the textile contribution decreases due to the transferring of load to the matrix via shear stress at the textile-to-mortar interface surface. Moreover, if the shear stress is considered constant along the whole length, the load distribution between matrix and textile presents the behaviour shown in **Figure 16**. In addition, assuming that the maximum matrix tensile stress is equal to its strength, the average bond stress (τ_m) can be evaluated as follows:

$$\tau_m = \frac{f_{t,matrix} \cdot A_{m,eq}}{\Delta x \cdot p_{Flax}} \tag{2}$$

where:

- $f_{t,matrix}$ represents the tensile strength of the mortar (assuming $f_{f,matrix}=1.1 \cdot f_{t,matrix}$);
- $A_{m,eq}$ is the equivalent cross-section area of the lime-based matrix;
- Δx is the distance between the crack and the section in which the tensile strength of the mortar is reached;
- p_{Flax} is the perimeter of the textile within the cross section.

The latter, is assumed to be equal to the product between the single yarn perimeter ($p_{Flax,yarn}$), the number of yarns comprised in the specimen transversal cross section ($n_{yarn,long}$) and the yarn length ($l_{yang,long}$):

$$p_{Flax} = p_{Flax,yarn} \cdot n_{yarn,long} \cdot l_{yarn,long} \tag{3}$$

The equivalent cross-section area of the mortar is calculated by considering the presence of both the transversal and longitudinal yarns:

$$A_{m,eq} = \frac{V_{TRM} - V_{Flax,textile}}{l_{TRM}} \quad (4)$$

where:

- V_{TRM} is the volume of the whole TRM composite specimen;
- $V_{Flax,textile}$ is the volume of the flax textile within the specimen,
- l_{TRM} is the length of the specimen.

The volume $V_{Flax,textile}$ is calculated as follows:

$$V_{Flax,textile} = A_{Flax,yarn} \cdot \left(n_{yarn,long} \cdot l_{yarn,long} + n_{yarn,trasv} \cdot l_{yarn,trasv} \right) \quad (5)$$

where:

- $A_{Flax,yarn}$ is the flax yarn transversal cross-section area;
- $n_{yarn,long}$ and $l_{yarn,long}$ are the number and the length of yarns comprised in the specimen transversal cross-section, respectively;
- $n_{yarn,transv}$ and $l_{yarn,transv}$ are, respectively, the number and the length of yarns comprised in the specimen longitudinal cross-section.

The value Δx is directly correlated to the distance between two consecutive cracks which was measured experimentally ($s_{m,exp}$):

$$\Delta x = \frac{s_{m,\exp}}{2} \quad (6)$$

Then, by substituting the eq.(6) in eq.(2) and by considering $s_{m,exp}$ as the average distance between two consecutive cracks observed in the tested specimens, an approximated estimation of the mean value of the maximum shear stress attainable at the textile-to-mortar interface is carried out (**Figure 17**). The average value of the distance between two consecutive cracks was computed as follows:

$$s_{m,\exp} = \frac{l_{TRM}}{n_{cracks} - 1} \quad (7)$$

where L_{TRM} is the initial specimen gauge length, and n_{crack} is the total number of cracks developed along the specimen.

It is worth mentioning that, with respect to the specimens of the series *TRM-1L*, the distance between the cracks was manually measured and only the specimens comprising two cracks were considered in the analysis.

All the values adopted for each series for the estimation of the bond strength are summarized in **Table 5**, while the resulting tm are plotted in **Figure 17**.

The histograms in **Figure 17** clearly show that the impregnation treatment performed on the Flax textile significantly improves the bond of the reinforcement embedded within the lime-based matrix. It was found that the τ_m is around three times higher in the case of impregnated TRM series. The quality of the proposed estimation is confirmed by the fact that the bond strength calculated with the above-mentioned procedure is almost independent from the reinforcement ratio (i.e., 1 or 2 layers of flax textiles) but it is governed by the adoption of the impregnation process.

4.CONCLUSIONS

This study presents the results of an experimental study aimed at investigating the influence of the reinforcement amount and the impregnation pre-treatment on the resulting performances of Textile Reinforced Mortars made of Flax textiles embedded within lime-based matrix.

The following main points can be concluded:

- the impregnation treatment performed on the dry textiles leads to improve the mechanical response of the reinforcement when subjected to tensile loads. In fact, although a small reduction of the tensile strength is registered for the impregnated textiles, the coated yarns are more stretched in comparison with the untreated textile and this confers an overall lower deformability to the Flax fabrics;

- the increasing of the reinforcement ratio improves the tensile response of the TRM. When untreated textiles are employed, the failure mode changes from *mode B* (textile slipping) to *mode A* (rupture of the textile) and by increasing the reinforcement amount, the number of cracks per linear meter increases while at the same time the crack width is reduced;

- the adoption of impregnated textiles increases the exploitation ratio leading to a significant optimization of the composite response. When the reinforcement ratio stays unchanged, the presence of coated flax fabric reduces the crack spacing as well as the crack width;

- the coating strategy adopted, although causing a general beneficial effect in the tensile behaviour of Flax-TRMs, leads to significant variability in the results. A standardisation method for the application of the coating on the textile is needed to obtain reliable results;

- the simplified approaches proposed herein for evaluating the crack width developments and the average bond strength furnish a comprehensive overview on the influence of either the reinforcement amount as well as the impregnation treatment on the resulting composite behavior;

- the analysis of the results allowed to estimate the average bond strength of the Flax textile embedded in a lime-based matrix: the results confirm the beneficial effect of the application of the impregnation pre-treatment.

The paper, by investigating the tensile behavior of Flax TRMs, shows that it is possible to obtain an overall improvement of the mechanical response of the composite system by mean of fiber treatment. However, it also emphasizes the importance of an accurate coating strategy in order to have reliable results. In this sense, the encouraging results of the study pave the way for further investigations aimed at defining a standardized textile impregnation procedure, allowing the application of a uniform coating layer with required thickness and stiffness. Moreover, research need to be pursued toward the investigation of the effect of the fiber treatment on other fundamental aspects, notably related to the durability and structural reliability of the composite system in the long-term.

5.ACKNOWLEDGEMENTS

The authors gratefully acknowledge the company INNOVATIONS s.r.l. for providing the materials tested in the experimental research presented in this paper.

REFERENCES

[1] H. Kaplan, H. Bilgin, S. Yilmaz, H. Binici, A. Öztas, Structural damages of L'Aquila (Italy) earthquake, Nat. Hazards Earth Syst. Sci., 10(3) (2010) 499-507. https://doi.org/10.5194/nhess-10-499-2010

[2] M. Indirli, L.A.S. Kouris, A. Formisano, R.P. Borg, F.M. Mazzolani, Seismic Damage Assessment of Unreinforced Masonry Structures After The Abruzzo 2009 Earthquake: The Case Study of the Historical Centers of L'Aquila and Castelvecchio Subequo, Int. J. Archit. Herit., 7(5) (2013) 536-578. https://doi.org/10.1080/15583058.2011.654050

[3] M. El Kadi, T. Tysmans, S. Verbruggen, J. Vervloet, M. De Munck, J. Wastiels, D. Van Hemelrijck, Experimental study and benchmarking of 3D textile reinforced cement composites, Cement Concr. Compos., 104 (2019)103352. https://doi:10.1016/j.cemconcomp.2019.103352

[4] L. Van Den Einde, L. Zhao, F. Seible, Use of FRP composites in civil structural applications, Constr. Build. Mater., 17(6) (2003) 389-403. https://doi.org/10.1016/S0950-0618(03)00040-0

[5] C.G. Papanicolaou, T.C. Triantafillou, K. Karlos, M. Papathanasiou, Textile-reinforced mortar (TRM) versus FRP as strengthening material of URM walls: in-plane cyclic loading, Mater. Struct., 40(10) (2007) 1081-1097. https://doi.org/10.1617/s11527-006-9207-8

[6] C. Papanicolaou, T. Triantafillou, M. Lekka, Externally bonded grids as strengthening and seismic retrofitting materials of masonry panels, Constr. Build. Mater., 2(25) (2011) 504-514. https://doi.org/10.1016/j.conbuildmat.2010.07.018

[7] X. Wang, C.C. Lam, V.P. Iu, Comparison of different types of TRM composites for strengthening masonry panels, Constr. Build. Mater., 219 (2019) 184–194. https://doi:10.1016/j.conbuildmat.2019.05.179

[8] M. Del Zoppo, M. Di Ludovico, A. Prota, Analysis of FRCM and CRM parameters for the in-plane shear strengthening of different URM types, Compos. Part B Eng., 171 (2019) 20–33. https://doi.org/10.1016/j.compositesb.2019.04.020

[9] L.A.S. Kouris, T.C. Triantafillou, State-of-the-art on strengthening of masonry structures with textile reinforced mortar (TRM), Constr. Build. Mater.,188 (2018) 1221–1233. https://doi.org/10.1016/j.conbuildmat.2018.08.039

[10] S. De Santis, F.G. Carozzi, G. de Felice, C. Poggi, Test methods for Textile Reinforced Mortar systems, Compos. Part B Eng., 127 (2017) 121–132. https://doi.org/10.1016/j.compositesb.2017.03.016

[11] F.G. Carozzi, A. Bellini, T. D'Antino, G. de Felice, F. Focacci, Ł. Hojdys, L. Laghi, E. Lanoye, F. Micelli, M. Panizza, C. Poggi, Experimental investigation of tensile and bond properties of Carbon-FRCM composites for strengthening masonry elements, Compos. Part B Eng., 128 (2017) 100–119. https://doi.org/10.1016/j.compositesb.2017.06.018

[12] S. De Santis, F. Ceroni, G. de Felice, M. Fagone, B. Ghiassi, A. Kwiecień, G.P. Lignola, M. Morganti, M. Santandrea, M.R. Valluzzi, A. Viskovic, Round Robin Test on tensile and bond behaviour of Steel Reinforced Grout systems, Compos. Part B Eng., 127 (2017) 100–120. https://doi.org/10.1016/j.compositesb.2017.03.052

[13] M. Saidi, X.H. Vu, E. Ferrier, Experimental and analytical analysis of the effect of water content on the thermomechanical behaviour of glass textile reinforced concrete at elevated temperatures, Cement Concr. Compos., (2020) 103690. https://doi:10.1016/j.cemconcomp.2020.103690

[14] M. Saidi, A. Gabor, Experimental analysis of the tensile behaviour of textile reinforced cementitious matrix composites using distributed fibre optic sensing (DFOS) technology, Constr. Build. Mater., 230 (2020) 117027. https://doi:10.1016/j.conbuildmat.2019.117027

[15] D.A. Strauss Rambo, F. de Andrade Silva, R.D. Toledo Filho, N. Ukrainczyk, E. Koenders, Tensile strength of a calcium-aluminate cementitious composite reinforced with basalt textile in a high-temperature environment, Cement Concr. Compos., 70 (2016) 183–193. https://doi:10.1016/j.cemconcomp.2016.04.006

[16] G. Ferrara, C. Caggegi, A. Gabor, E. Martinelli, Experimental Study on the Adhesion of Basalt Textile Reinforced Mortars (TRM) to Clay Brick Masonry: The Influence of Textile Density, Fibers, 7(12) (2019) 103. https://doi:10.3390/fib7120103

[17] C. Caggegi, F.G. Carozzi, S. De Santis, F. Fabbrocino, F. Focacci, Ł. Hojdys, E. Lanoye, L. Zuccarino, Experimental analysis on tensile and bond properties of PBO and aramid fabric reinforced cementitious matrix for strengthening masonry structures, Compos. Part B Eng., 127 (2017)175–195. https://doi.org/10.1016/j.compositesb.2017.05.048

[18] L.H. Sneed, T. D'Antino, C. Carloni, C. Pellegrino, A comparison of the bond behavior of PBO-FRCM composites determined by double-lap and single-lap shear tests, Cement Concr. Compos., 64 (2015) 37–48. https://doi:10.1016/j.cemconcomp.2015.07.007

[19] S. Yin, L. Jing, M. Yin, B. Wang, Mechanical properties of textile reinforced concrete under chloride wet-dry and freeze-thaw cycle environments, Cement Concr. Compos., 96 (2019) 118–127. https://doi:10.1016/j.cemconcomp.2018.11.020

[20] J. Claramunt, M. Ardanuy, J.A. García-Hortal, R.D.T. Filho, The hornification of vegetable fibers to improve the durability of cement mortar composites, Cement Concr. Compos., 33(5) (2011) 586–595. https://doi:10.1016/j.cemconcomp.2011.03.003

[21] J. Donnini, Durability of glass FRCM systems: Effects of different environments on mechanical properties, Compos. Part B Eng., 174 (2019) 107047. https://doi.org/10.1016/j.compositesb.2019.107047

[22] L. Coppola *et al.*, Binders alternative to Portland cement and waste management for sustainable construction-part 1, J. Appl. Biomater. Funct. Mater., 16(3) (2018) 186–202. https://doi:10.1177/2280800018782845

[23] L. Coppola *et al.*, Binders alternative to Portland cement and waste management for sustainable construction – Part 2, J. Appl. Biomater. Funct. Mater., 16(4) (2018) 207–221. https://doi.org/10.1177/2280800018782852

[24] C. Faella, C. Lima, E. Martinelli, M. Pepe, R. Realfonzo, Mechanical and durability performance of sustainable structural concretes: An experimental study, Cement Concr. Compos., 71 (2016) 85–96. https://doi.org/10.1016/j.cemconcomp.2016.05.009

[25] M. Bassani, L. Tefa, B. Coppola, P. Palmero, Alkali-activation of aggregate fines from construction and demolition waste: Valorisation in view of road pavement subbase applications, J. Clean. Prod., 234 (2019) 71–84. https://doi:10.1016/j.jclepro.2019.06.207

[26] M.P.M. Dicker, P.F. Duckworth, A.B. Baker, G. Francois, M.K. Hazzard, P.M. Weaver, Green composites: A review of material attributes and complementary applications, Compos. Part Appl. Sci. Manuf., 56 (2014) 280–289. https://doi.org/10.1016/j.compositesa.2013.10.014

[27] R. Codispoti, D.V. Oliveira, R.S. Olivito, P.B. Lourenço, R. Fangueiro, Mechanical performance of natural fiber-reinforced composites for the strengthening of masonry, Compos. Part B Eng., 77 (2015) 74–83. https://doi.org/10.1016/j.compositesb.2015.03.021

[28] B. Zukowski, E.R.F. dos Santos, Y.G. dos Santos Mendonça, F. de Andrade Silva, R.D. Toledo Filho, The durability of SHCC with alkali treated curaua fiber exposed to natural weathering, Cement Concr. Compos., 94 (2018) 116–125. https://doi:10.1016/j.cemconcomp.2018.09.002

[29] O. Onuaguluchi, N. Banthia, Plant-based natural fibre reinforced cement composites: A review, Cement Concr. Compos., 68 (2016) 96–108. https://doi:10.1016/j.cemconcomp.2016.02.014

[30] G. Ferrara, M. Pepe, E. Martinelli, R.D. Tolêdo Filho, Influence of an Impregnation Treatment on the Morphology and Mechanical Behaviour of Flax Yarns Embedded in Hydraulic Lime Mortar, Fibers. 7(4) (2019) 30. https://doi.org/10.3390/fib7040030

[31] C.B. de Carvalho Bello, I. Boem, A. Cecchi, N. Gattesco, D.V. Oliveira, Experimental tests for the characterization of sisal fiber reinforced cementitious matrix for strengthening masonry structures, Constr. Build. Mater., 219 (2019) 44–55. https://doi.org/10.1016/j.conbuildmat.2019.05.168

[32] C. Menna, D. Asprone, M. Durante, A. Zinno, A. Balsamo, A. Prota, Structural behaviour of masonry panels strengthened with an innovative hemp fibre composite grid, Constr. Build. Mater., 100 (2015) 111–121. https://doi.org/10.1016/j.conbuildmat.2015.09.051

[33] G. Ferrara, C. Caggegi, E. Martinelli, A. Gabor, Shear capacity of masonry walls externally strengthened using Flax-TRM composite systems: experimental tests and comparative assessment, Constr. Build. Mater., 261 (2020) 120490. https://doi.org/10.1016/j.conbuildmat.2020.120490

[34] O.A. Cevallos, R.S. Olivito, R. Codispoti, L. Ombres, Flax and polyparaphenylene benzobisoxazole cementitious composites for the strengthening of masonry elements subjected to eccentric loading, Compos. Part B Eng., 71 (2015) 82–95. https://doi.org/10.1016/j.compositesb.2014.10.055

[35] R. S. Olivito, O.A. Cevallos, A. Carrozzini, Development of durable cementitious composites using sisal and flax fabrics for reinforcement of masonry structures, Mater. Des., 57 (2014) 258–268. https://doi.org/10.1016/j.matdes.2013.11.023

[36] O.A. Cevallos, R.S. Olivito, Effects of fabric parameters on the tensile behaviour of sustainable cementitious composites, Compos. Part B Eng., 69 (2015) 256–266. https://doi.org/10.1016/j.compositesb.2014.10.004

[37] R.D. Toledo Filho, K. Scrivener, G.L. England, K. Ghavami, Durability of alkali-sensitive sisal and coconut fibres in cement mortar composites, Cement Concrete Comp., 22 (2000) 127–143. https://doi.org/10.1016/S0958-9465(99)00039-6

[38] G. Ferrara, B. Coppola, L. Di Maio, L. Incarnato, E. Martinelli, Tensile strength of flax fabrics to be used as reinforcement in cement-based composites: experimental tests under different environmental exposures, Compos. Part B Eng.,168 (2019) 511–523. https://doi:10.1016/j.compositesb.2019.03.062

[39] S.R. Ferreira, F. de A. Silva, P.R.L. Lima, R.D. Toledo Filho, Effect of fiber treatments on the sisal fiber properties and fiber–matrix bond in cement based systems, Constr. Build. Mater., 101 (2015) 730–740. https://doi.org/10.1016/j.conbuildmat.2015.10.120

[40] Zukowski B, de Andrade Silva F, R.D. Toledo Filho, Design of strain hardening cement-based composites with alkali treated natural curauá fiber. Cememnt Concr. Compos., 89 (2018) 150–159. https://doi:10.1016/j.cemconcomp.2018.03.006

[41] Technical sheet (*in Italian*) available at www.fidiaglobalservice.com/ita/materiali_schede/FIDFLAX%20GRID%20300%20HS20.pdf (accessed on 29.12.2020)

[42] Technical sheet available at www.nitriflex.com.br/storage/produtos/N-218%20EPA%20Rev07.pdf (accessed on 29.12.2020)

[43] ISO 13934-1:2013. Textiles-Tensile properties of fabrics. Part 1: Determination of maximum force and elongation at maximum force using strip method.

[44] Technical sheet (*in Italian*) available at www.fidiaglobalservice.it/ita/materiali_schede/FIDCALX_NHL5.pdf (accessed on 29.12.2020)

[45] EN 1015-3: 1999. Methods of Test Mortar for Masonry. Determination of Consistence of Fresh Mortar (by Flow Table); European Committee for Standardization: Brussels, Belgium, 1999.

[46] EN 196-1:1994. Methods of Testing Cement—Part 1: Determination of Strength; European Committee for Standardization: Brussels, Belgium, 1994.

[47] RILEM Technical Committee (Brameshuber W), Recommendation of RILEM TC 232-TDT: test methods and design of textile reinforced concrete. Uniaxial tensile test: test method to determine the load bearing behavior of tensile specimens made of textile reinforced concrete, Mater. Struct., 49 (2016) 4923-4927. https://doi.org/10.1617/s11527-016-0839-z

[48] M. Messori, A, Nobili, C. Signorini, A. Sola, Mechanical performance of epoxy coated AR-glass fabric Textile Reinforced Mortar: Influence coating thickness and formulation. Compos. Part B Eng., 149 (2018) 135–143. https://doi.org/10.1016/j.compositesb.2018.05.023

[49] International Federation for Structural Concrete (fib). (2013). The fib Model Code for Concrete Structures 2010.

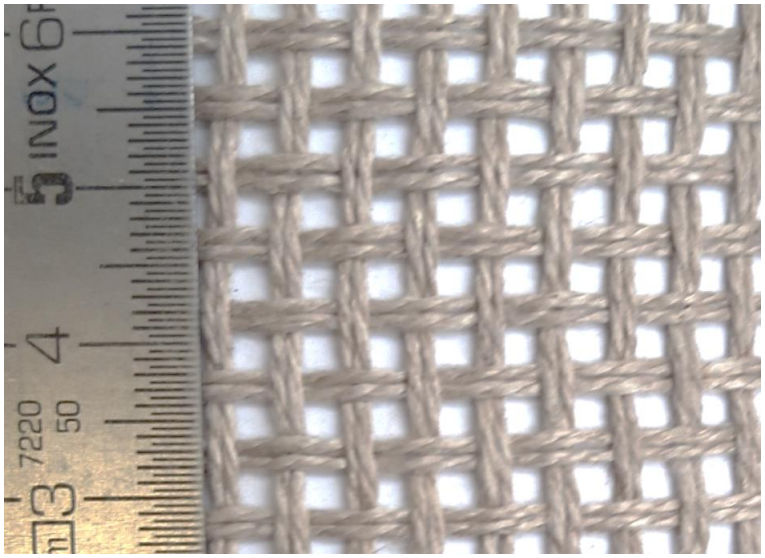

Figure 1. *Bi-directional flax textile employed in this study.*

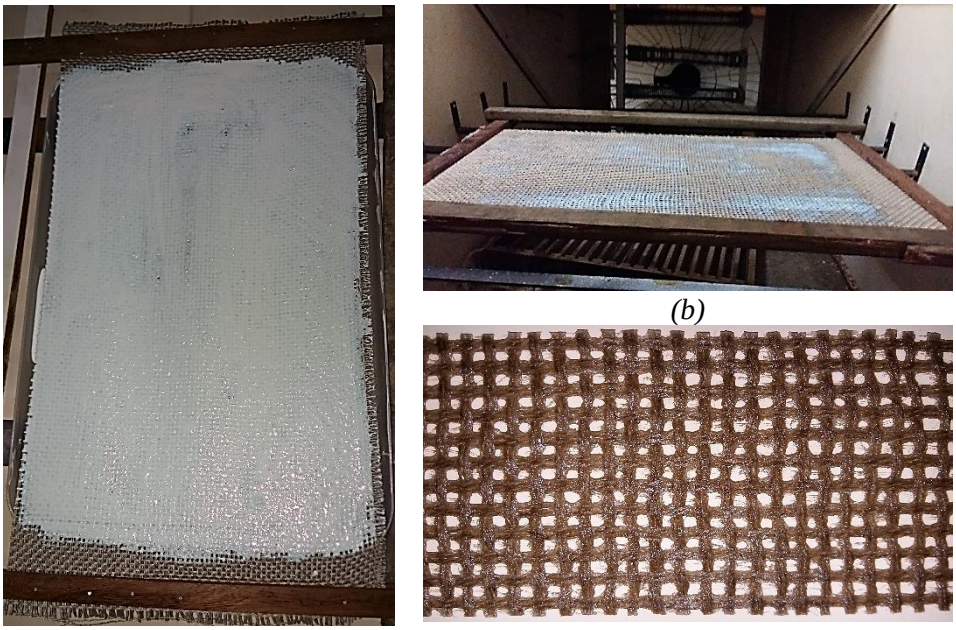

(a) *(b)* *(c)*

Figure 2. *Textile impregnation treatment: (a) polymer coating application, (b) drying of the textile and (c) impregnated flax strip.*

Figure 3. *Tensile test set-up for Flax Textile*.

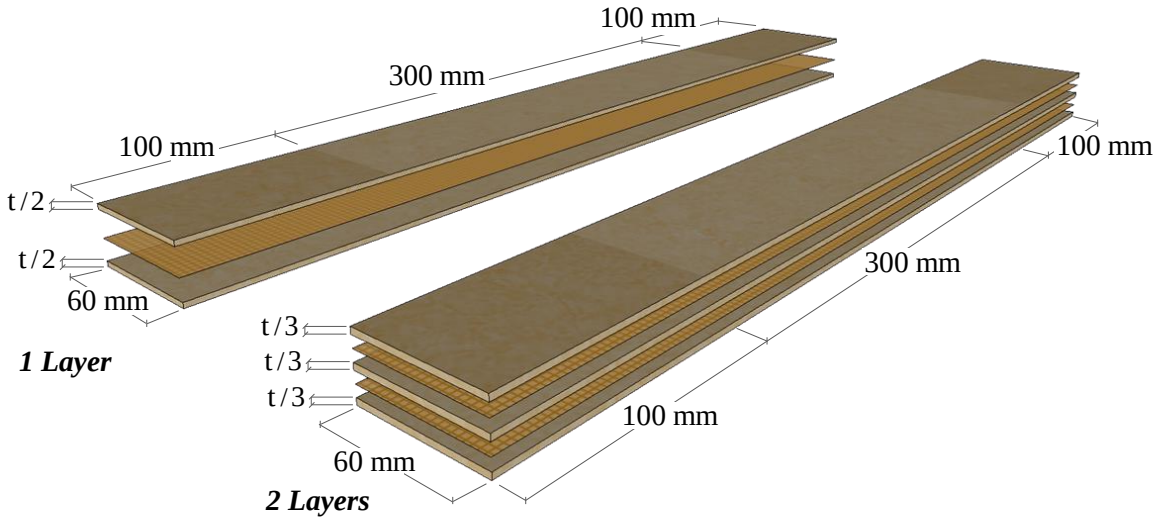

Figure 4. *Schematic representation of the produced Flax-TRMs.*

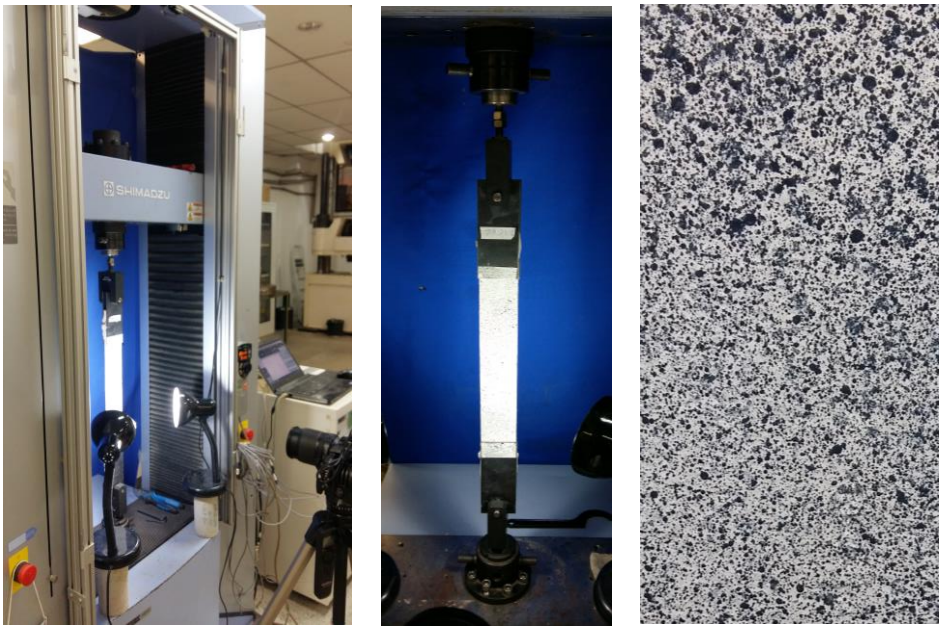

(a) *(b)* *(c)*

Figure 5. *Tensile test setup for Flax-TRM composites.*

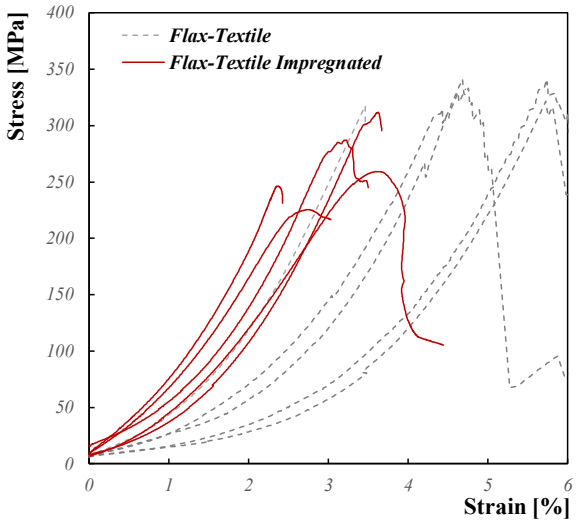

Figure 6. *Stress-strain response of Flax-Textile and Impregnated Flax-Textile strips.*

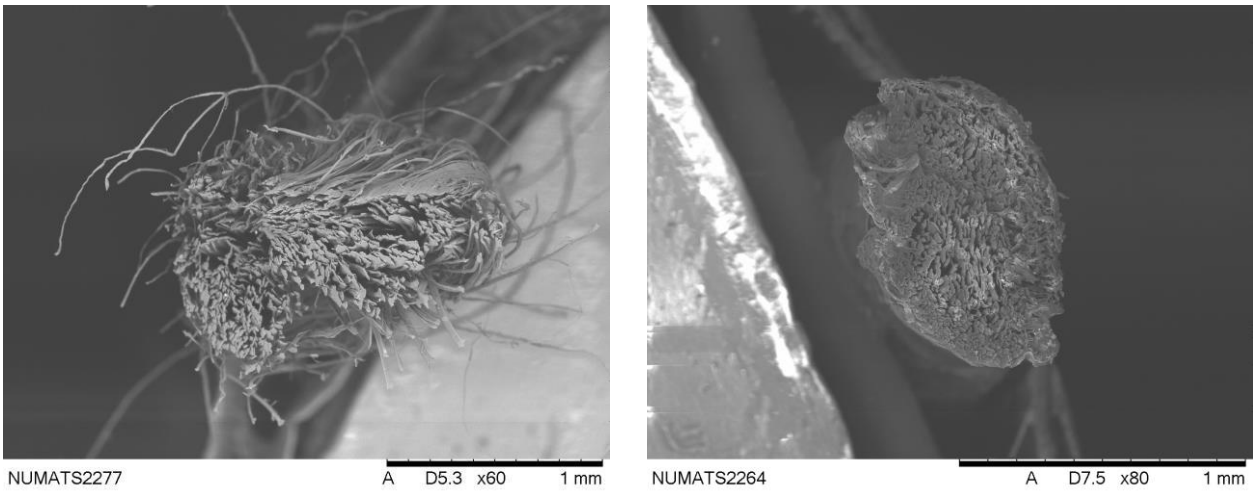

(a) *(b)*

Figure 7. *Representative SEM images for (a) non impregnated and (b) impregnated flax yarns subjected to tensile tests.*

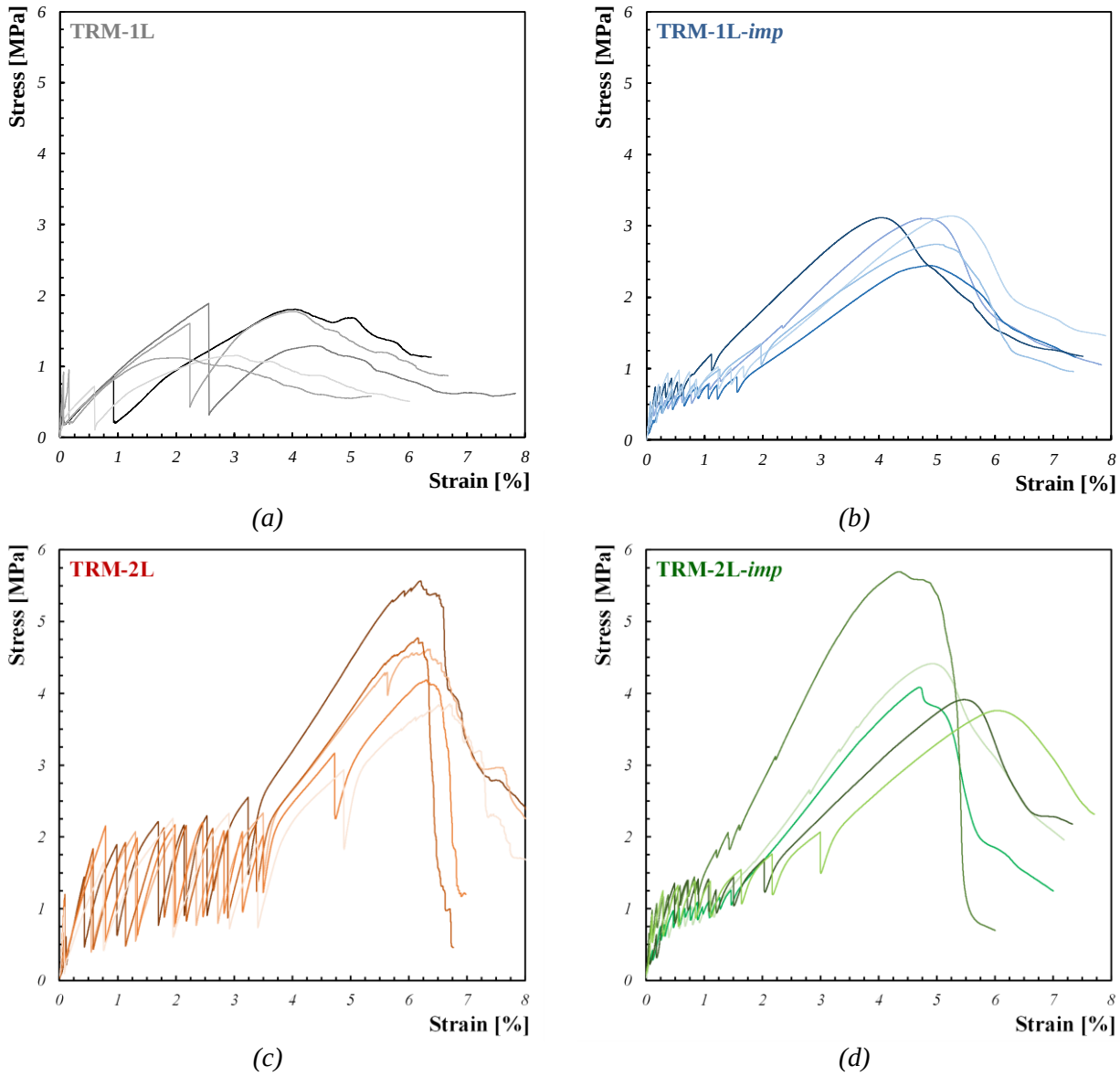

Figure 8. *Stress-strain response for (a) Flax TRM-1L, (b) Flax TRM-1L-imp, (c) Flax TRM-2L and (d) Flax TRM-2L-imp.*

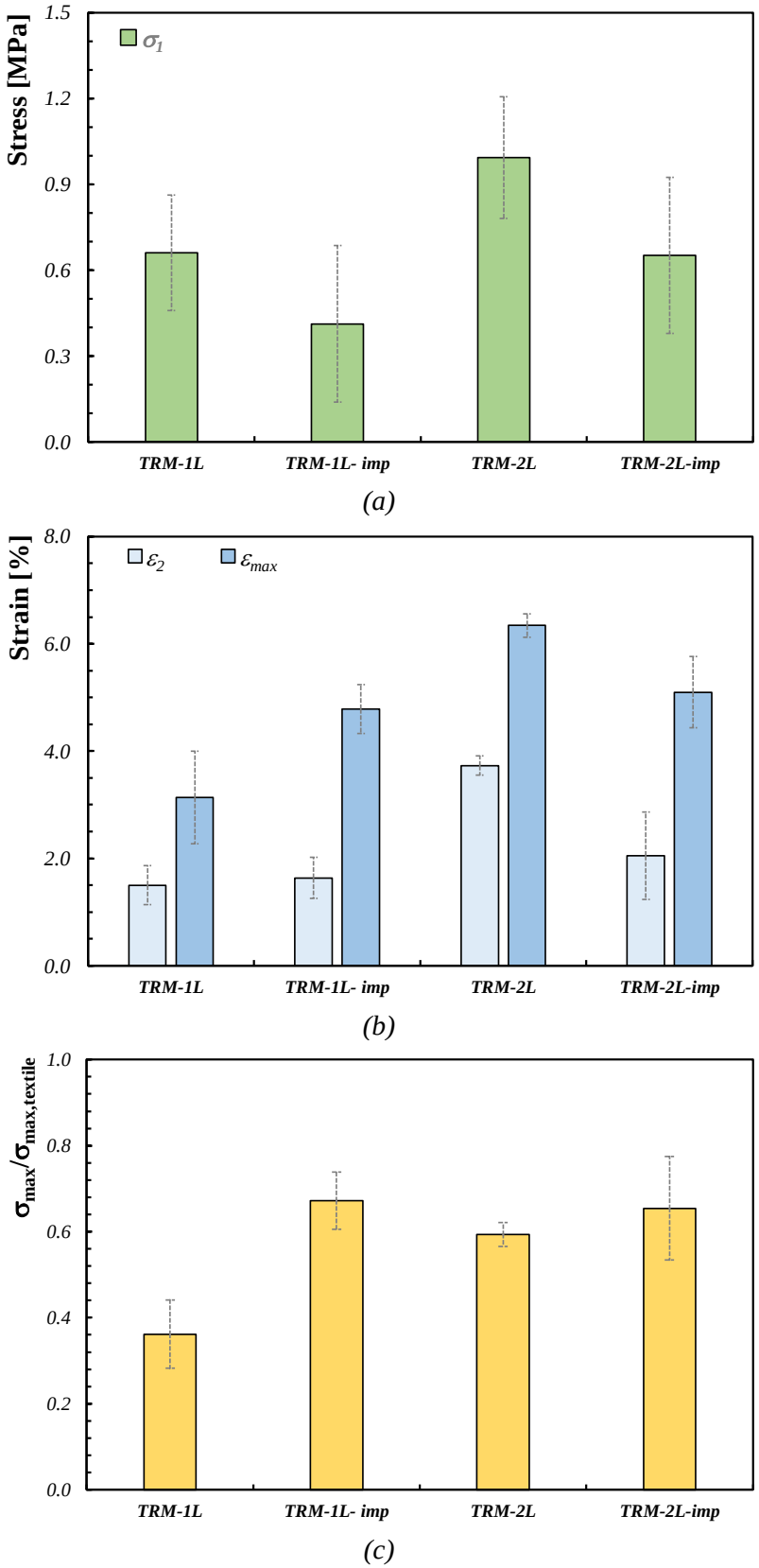

Figure 9: *Average values for (a) σ_1, (b) ε_2 & ε_{max} and (c) fibers exploitation ratio.*

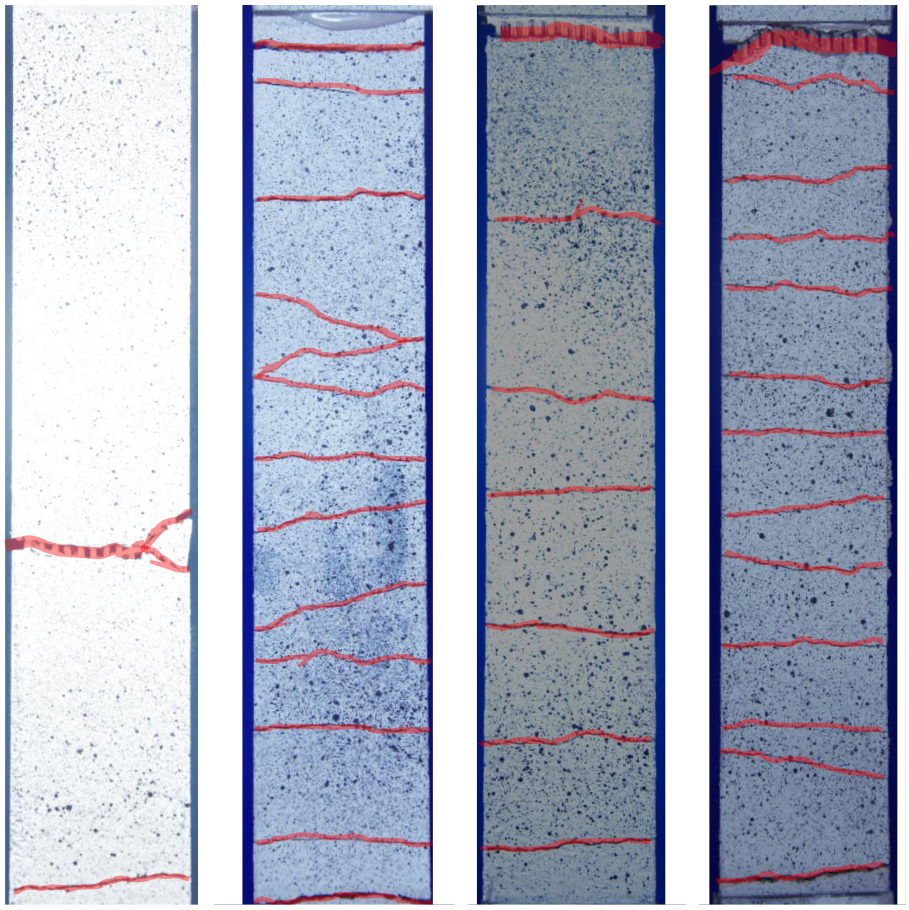

(a) *(b)* *(c)* *(d)*

Figure 10. *Crack pattern of representative specimens of (a)TRM-1L, (b) TRM-1L-imp, (c) TRM-2L, (d) TRM-2L-imp.*

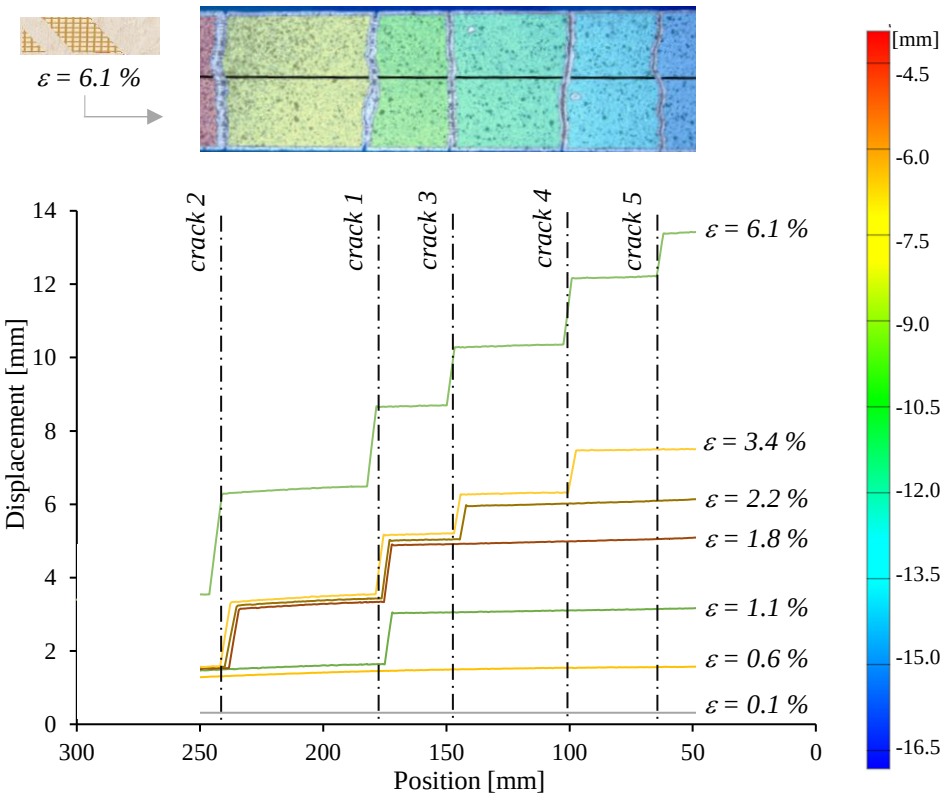

Figure 11. *DIC analysis for cracks analysis performed on Flax TRM.*

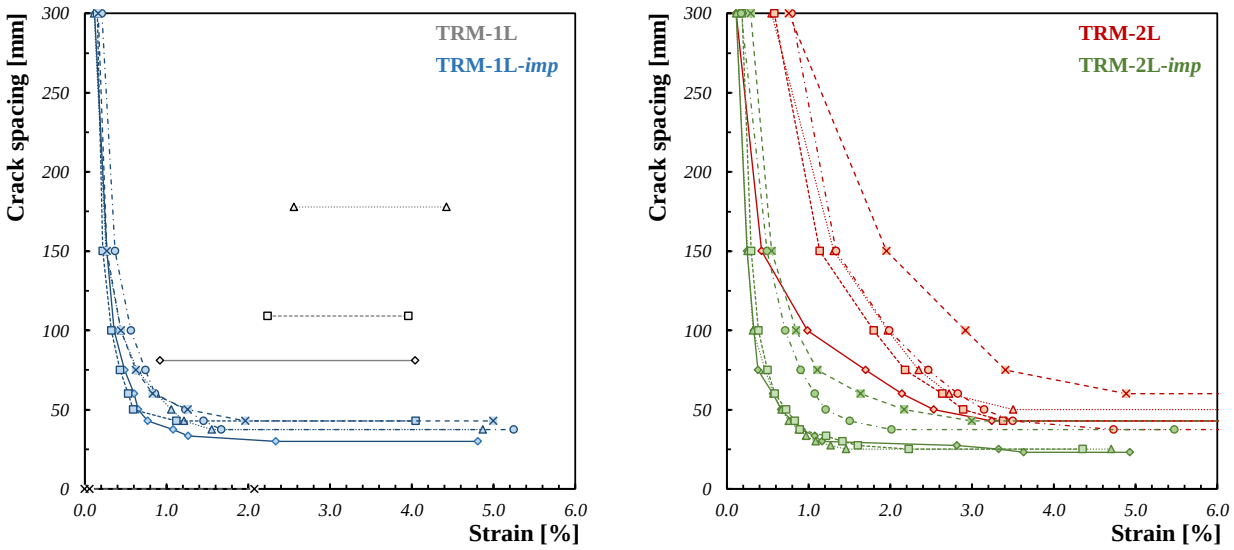

Figure 12. *Crack spacing vs strain curves for (a) Flax TRM-1L & Flax TRM-1L-imp and (b) Flax TRM-2L & Flax TRM-2L series.*

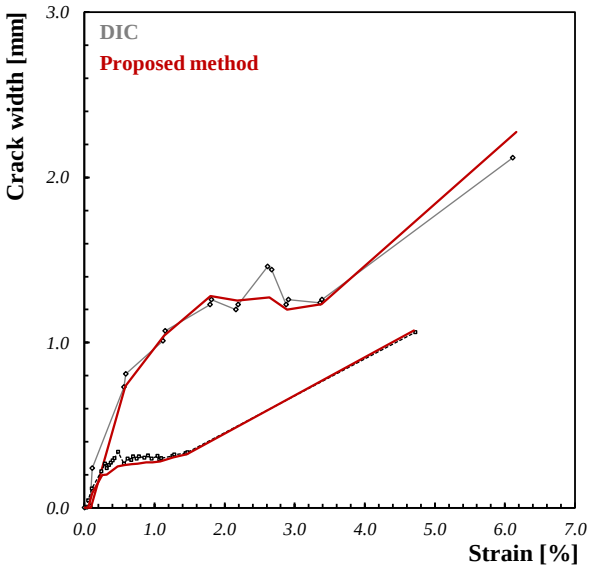

Figure 13. *Crack width evaluation: comparison between the proposed method vs DIC analysis.*

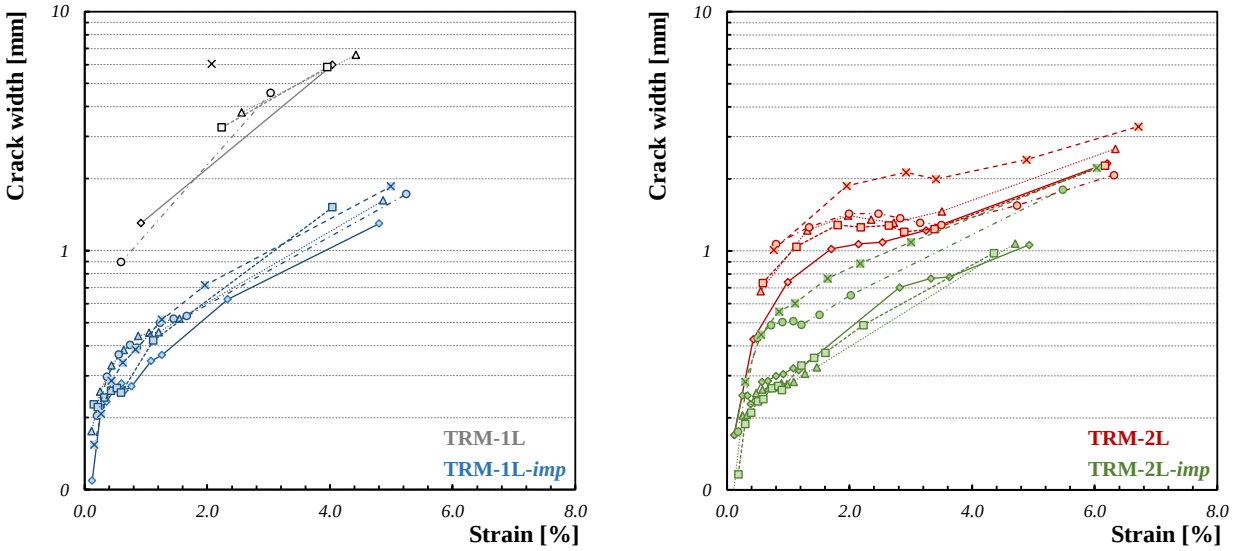

Figure 14. *Crack width vs strain curves for (a) Flax TRM-1L & Flax TRM-1L-imp and (b) Flax TRM-2L & Flax TRM-2L series.*

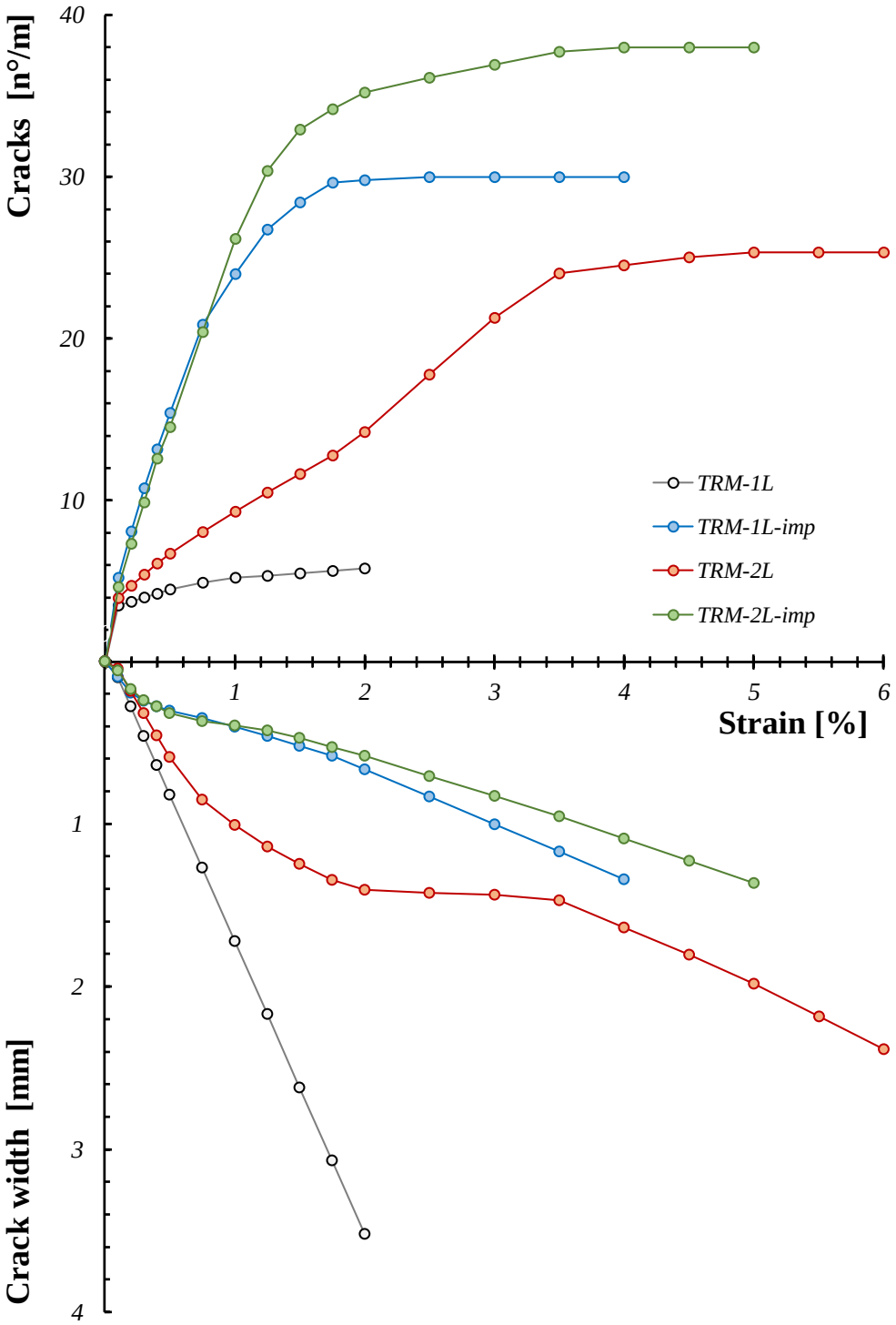

Figure 15. *Average number of cracks and crack width for Flax TRM composites.*

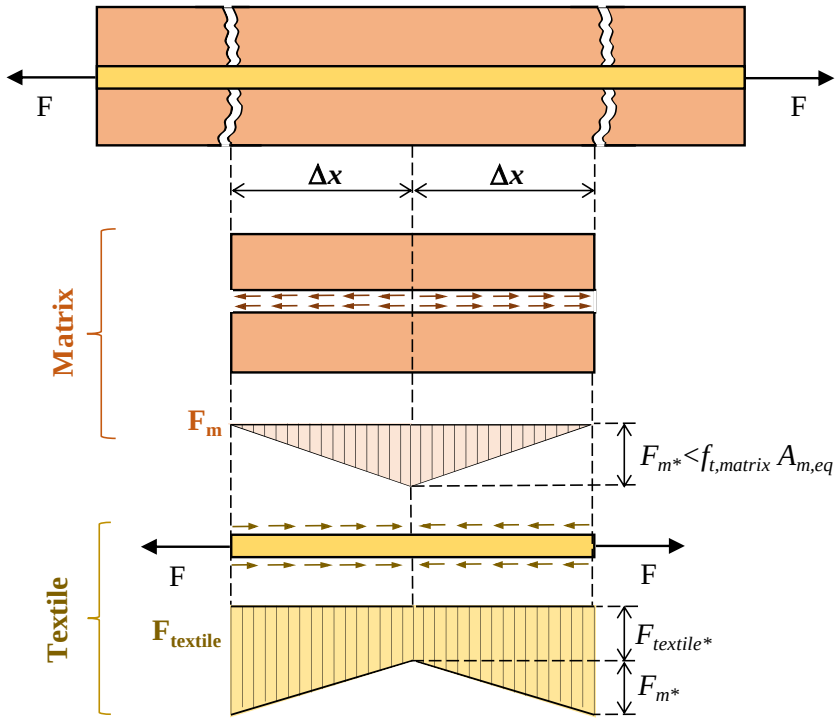

Figure 16. *Stress distribution in cracked TRM.*

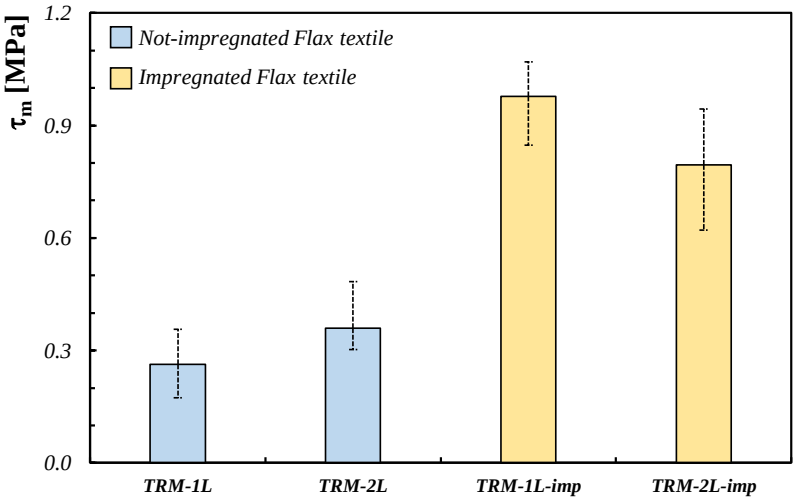

Figure 17. *Estimation of the average bond strength.*

Table 1. *Properties of hydraulic lime-based mortar*.

Property	***symbol***	***value***	***n° tests***	***cv***
Spreading [mm]	***d****	230	*4*	*4%*
Flexural strength [MPa]	f_f	4.2	*12*	*11%*
Compressive strength [MPa]	f_c	9.5	*24*	*12%*

***Table 2**. Flax TRM composites for tensile tests: relevant properties of the different series.*

Series	***n. of spec.***	***textile***	***textile layer***	t_{mean} ***[mm]***	A_{text} ***[mm²]***	ρ ***[%]***
TRM-1L	5	Flax	1	7.9	6.1	1.3
TRM-1L-imp	5	Impregnated Flax	1	6.3	6.1	1.6
TRM-2L	5	Flax	2	8.8	12.2	2.3
TRM-2L-imp	5	Impregnated Flax	2	8.1	12.2	2.5

***Table 3**. Properties of Flax Textile and Impregnated Flax Textile strips tested in tension.*

Series	P_{max}		δ_{max}		σ_{max}		ε_{max}		***E***	
	[N]	***cv***	***[mm]***	***cv***	***[MPa]***	***cv***	***[%]***	***cv***	***[GPa]***	***cv***
Dry Flax Strip	2024	*3%*	9.7	*19%*	331	*3%*	4.9	*19%*	12.5	*6%*
Imp. Flax Strip	1627	*13%*	6.2	*18%*	266	*13%*	3.1	*18%*	12.4	*14%*

***Table 4**. Average properties of Flax TRMs under tensile loads.*

Series	P_{max}		d_{max}		σ_{max}		ε_{max}		$\sigma_{max,text}$		n_{cracks}		Failure mode
	[N]	cv	[mm]	cv	[MPa]	cv	[%]	cv	[MPa]	cv	min	max	
TRM-1L	732	*22%*	9.4	*27%*	1.5	*24%*	3.1	*27%*	120	*22%*	1	2	B
TRM-1L- imp	1094	*10%*	14.3	*10%*	2.9	*11%*	4.8	*10%*	179	*10%*	8	11	A
TRM-2L	2402	*5%*	19.0	*3%*	4.6	*14%*	*6.3*	*3%*	196	*5%*	6	8	A
TRM-2L-imp	2129	*18%*	15.3	*13%*	4.4	*18%*	5.1	*13%*	174	*18%*	8	14	A

***Table 5**. Parameters the evaluation of τ_m.*

Series	$p_{Flax\ yarn}$ ***[mm]***	$n_{yarn,long}$	$A_{m,eq}$ ***[mm^2]***	$s_{m,exp}$ ***[mm]***	***cv***
TRM-1L	4.9	24	463.8	95	21%
TRM-1L-imp	3.1	24	366.6	38	14%
TRM-2L	4.9	48	504.1	47	19%
TRM-2L-imp	3.1	48	463.3	31	29%